

Journal of Applied Remote Sensing

RemoteSensing.SPIEDigitalLibrary.org

Ultraviolet beam splitter characterization for use in a CubeSat optical system

Bruce A. Fritz
Andrew W. Stephan
Peter W. Walker
Charles M. Brown
Andrew C. Nicholas
Kenneth F. Dymond
Scott A. Budzien
Peter J. Marquis
Ted T. Finne
Kenneth D. Wolfram

SPIE.

Bruce A. Fritz, Andrew W. Stephan, Peter W. Walker, Charles M. Brown, Andrew C. Nicholas, Kenneth F. Dymond, Scott A. Budzien, Peter J. Marquis, Ted T. Finne, Kenneth D. Wolfram, "Ultraviolet beam splitter characterization for use in a CubeSat optical system," *J. Appl. Remote Sens.* **13**(3), 032503 (2019), doi: 10.1117/1.JRS.13.032503.

Ultraviolet beam splitter characterization for use in a CubeSat optical system

Bruce A. Fritz,^{a,*} Andrew W. Stephan,^b Peter W. Walker,^c
Charles M. Brown,^b Andrew C. Nicholas,^b Kenneth F. Dymond,^b
Scott A. Budzien,^b Peter J. Marquis,^b Ted T. Finne,^b
and Kenneth D. Wolfram^d

^aNational Research Council Postdoctoral Research Associate Resident at the U.S. Naval Research Laboratory, Washington, DC, United States

^bU.S. Naval Research Laboratory, Space Science Division, Washington, DC, United States

^cComputational Physics Inc., Springfield, Virginia, United States

^dPraxis, Inc., Arlington, Virginia, United States

Abstract. The U.S. Naval Research Laboratory (NRL) has developed the Triple Tiny Ionospheric Photometer (Tri-TIP), an ultraviolet remote-sensing instrument based on the TIP. Tri-TIP measures emissions of atomic oxygen (OI 135.6 nm) to determine plasma density in the nighttime ionosphere. The Tri-TIP design shrinks TIP to a 1U CubeSat form-factor and simplifies the mechanical design with a three-channel photometer system to isolate the target wavelength without a filter wheel. A heated strontium fluoride (SrF₂) filter eliminates incoming light at wavelengths shorter than 135.6 nm. The filtered light is divided between two matched photometers by a beam splitter with a magnesium fluoride coating over aluminum (AlMgF₂) deposited on 50% of the surface in a polka-dot pattern. The third photometer monitors dark count noise for later subtraction. One Tri-TIP configuration uses a beam splitter with a sapphire (Al₂O₃) substrate, which is opaque to wavelengths shorter than ~140 nm, to later subtract contaminating emissions at wavelengths longer than 140 nm. A second Tri-TIP configuration uses a MgF₂ substrate beam splitter to simultaneously measure OI 135.6 nm from two adjacent fields-of-view. The performance of both beam splitters has been tested at NRL, and the results are presented. © The Authors. Published by SPIE under a Creative Commons Attribution 4.0 Unported License. Distribution or reproduction of this work in whole or in part requires full attribution of the original publication, including its DOI. [DOI: [10.1117/1.JRS.13.032503](https://doi.org/10.1117/1.JRS.13.032503)]

Keywords: space optics; far ultraviolet; airglow; photometry; optical design; optical testing.

Paper 190237SS received Apr. 1, 2019; accepted for publication May 23, 2019; published online Jun. 11, 2019.

1 Introduction

Robust beam splitters in the vacuum ultraviolet (VUV) wavelength range are challenging to manufacture given the limited number of suitable substrates and coating materials normally available.^{1,2} Commercially available VUV bandpass filters typically have a full-width half-maximum of 20 nm or more, which makes distinguishing closely spaced emission lines from one another difficult. The Space Science Division at the U.S. Naval Research Laboratory (NRL) has adopted a simple, polka-dot patterned beam splitter for use in a CubeSat sized space instrument (10 cm × 10 cm × 10 cm) made from commercially available materials and processes. Selected transmitting substrates have been coated with a pattern of reflective spots covering 50% of the surface area. This article describes the motivation, design, characterization, and implementation of VUV beam splitters with a polka-dot reflective pattern.

The lower atmosphere on Earth completely absorbs light at far ultraviolet (FUV) wavelengths. Space-based remote sensing of the upper atmosphere is therefore well suited for the FUV spectral regime due to the lack of background emission from the Earth's surface and lower atmosphere. The *F* region of the ionosphere, from ~150 to 500 km in altitude, emits light at

*Address all correspondence to Bruce A. Fritz, E-mail: bruce.fritz.ctr@nrl.navy.mil

several discrete FUV wavelengths. At night, these emissions are known as nightglow and are often used to characterize the physical state of the ionosphere.³ NRL has developed a class of compact, high-sensitivity, remote sensing instruments to measure FUV nightglow and monitor the density and structure of the ionosphere.^{3,4}

The Tiny Ionospheric Photometer (TIP) was first developed by NRL to monitor FUV emissions of atomic oxygen in the ionosphere as part of the Constellation Observing System for Meteorology, Ionosphere, and Climate (COSMIC) mission, also known as the Formosa Satellite Mission #3 (FORMOSAT-3).^{4,5} The *F* region ionosphere is composed predominantly of electrons and O⁺ ions (~99%) with minor populations of O₂⁺, N₂⁺, N⁺, H⁺, He⁺, and NO⁺ ions. Nightglow is primarily produced by the decay of ionospheric plasma, especially via radiative recombination (between ions and electrons) and mutual neutralization (between positive and negative ions). In particular, the recombination of O⁺ with electrons produces neutral oxygen atoms in an excited electronic state. Excited oxygen atoms release photons as they return to the ground state and emit two of the brightest features in Earth's FUV nightglow spectrum. One feature, a triplet at 130.2, 130.4, and 130.6 nm (hereafter referred to as OI 130.4 nm), is difficult to analyze because high levels of atmospheric absorption make it optically thick. The other feature, a spin-forbidden doublet at 135.6 and 135.8 nm (referred to as OI 135.6 nm), is optically thin and was used by TIP to determine the plasma density of the *F* region along the spacecraft nadir.⁴

Narrow bandpass, VUV filters with sufficient out-of-band rejection to suppress nearby bright emission lines like hydrogen Lyman- α (121.6 nm) and OI 130.4 nm are difficult to create and use.^{1,2} Filters produced using multilayer techniques have shown promise but are not widely commercially available and still may not provide the required 99% out-of-band rejection at 130.4 nm.⁶ TIP uses a strontium fluoride (SrF₂) long-pass filter that is heated to 100°C to shift the cutoff wavelength and attenuate light at wavelengths shorter than ≈ 132.5 nm.⁶ The TIP detector is a Hamamatsu photomultiplier tube (PMT) with a cesium iodide (CsI) photocathode.⁷ The radiant sensitivity and quantum efficiency of CsI photocathodes are high at 135.6 nm and have a long wavelength cutoff near 200 nm.⁸ Earth's nightglow is generally devoid of bright emission features at wavelengths from 140 to 200 nm, which means the bandpass provided by the CsI photocathode response and the SrF₂ filter cutoff effectively isolates the OI 135.6-nm emission.³

The TIP sensitivity was designed to be greater than 150 counts per second per Rayleigh (cts/s/R), based on expected nightglow signals of 0.1 to 10 R emitted by ionospheres with peak electron densities of $n_e = 1 \times 10^5$ cm⁻³ to $n_e = 1 \times 10^6$ cm⁻³.⁷ Testing demonstrated that the instrument far exceeded the minimum sensitivity requirement.^{5,9} Some TIP signals from the COSMIC mission, however, can be correlated with longer wavelength city lights and moonlight scattered from clouds, complicating the analysis of the data.⁵ CsI photocathodes like those used in the TIP PMTs are supposed to be "solar blind" but have shown a small sensitivity beyond the 200-nm cutoff due to various physical effects.¹⁰ Relative to the dim nightglow features targeted by TIP, extremely bright features at wavelengths longer than 200 nm were sometimes strong enough to overwhelm the FUV emissions despite the low PMT sensitivity to the out-of-band wavelengths. This "red leak" of the PMT used in TIP was addressed in a follow-on mission, the GPS Radio Occultation and Ultraviolet Photometry—co-located (GROUP-C) experiment on the International Space Station.¹¹ The GROUP-C TIP added a long-pass sapphire (Al₂O₃) filter with a cutoff at ≈ 140 nm to measure the long wavelength background, so it could be subtracted from the FUV signal. However, the mechanical filter wheel used to cycle the sapphire filter in and out of the optical path adds the complication of moving parts and creates disturbance torques that must be accounted for by smaller spacecraft like CubeSats. The filter wheel also introduces some space-time ambiguity due to the need to alternate measurements between the SrF₂ and Al₂O₃ filters, which can complicate the subtraction of city light and other visible light contamination.

Eliminating the filter wheel to simplify the mechanical design and improve measurement cadence was a driving requirement to develop the Tri-TIP instrument as part of the Coordinated Ionospheric Reconstruction CubeSat Experiment (CIRCE).¹² Rather than a mechanical filter system, Tri-TIP uses multiple PMTs to simultaneously measure the effects of both the red leak and dark noise in the system. A VUV-grade sapphire beam splitter distributes the incoming signal

between a UV PMT and a red leak PMT, while a third PMT is totally covered to characterize dark counts.¹³ The red leak PMT and dark count PMT signals are later subtracted from the UV PMT to isolate OI 135.6 nm.¹⁴ The red leak and UV PMTs will be matched based on laboratory-tested sensitivities prior to flight.

A second, similar implementation of Tri-TIP has also been developed as a limb sounder for CIRCE to measure OI 135.6-nm emissions above the Earth's limb. The potential for long wavelength contamination is not present when viewing directions above the Earth's surface, which frees the red leak PMT for use as a second UV PMT. As a result, the limb sounding Tri-TIP can simultaneously view the Earth's nightglow along two lines of sight that pass above the Earth's limb at different altitudes or tangent heights. The Al_2O_3 beam splitter is replaced with a VUV-grade MgF_2 beam splitter that then divides the signal without eliminating OI 135.6 nm. This version of Tri-TIP uses narrow slits at the focal points to select two narrow altitude ranges.¹⁵

The CIRCE mission employs four Tri-TIP units across two 6U CubeSats flying in a lead/trail formation. One Tri-TIP will observe the nadir and two will view a common volume at 45 deg to the local horizon, all three of which will use the sapphire beam splitter for red leak correction. The fourth Tri-TIP (the Limb Sounder) will view above the Earth's limb to measure two separate tangent altitudes. This article focuses on the characterization of the VUV beam splitters that divide the observed signal between the two illuminated PMTs within the Tri-TIP instrument. First, Sec. 2 will provide a brief description of the Tri-TIP instrument for context. Section 3 will then provide an explanation of the methodology used in the tests, including the testing equipment and setup. Last, Sec. 4 will discuss the results of the beam splitter tests and how this component will be used to produce the desired instrument passband. The Tri-TIP instrument will be the first to use a VUV beam splitter in an optical system to help produce a narrow effective passband with strong out-of-band rejection for use in a 1U CubeSat instrument.

2 Instrumentation

The Tri-TIP instrument is designed to fit within a 1U CubeSat form factor. Figure 1 shows an isometric external view of the full Tri-TIP assembly (a) and the internal optical path through the Tri-TIP and into the detectors (b). Light enters Tri-TIP through a simple, two-vane baffle. An off-axis parabolic (OAP) mirror with a reflective coating of MgF_2 over Aluminum (~ 110 nm Al plus ~ 25 nm MgF_2) focuses the light through a heated strontium fluoride (SrF_2) filter.¹⁶ Heating the

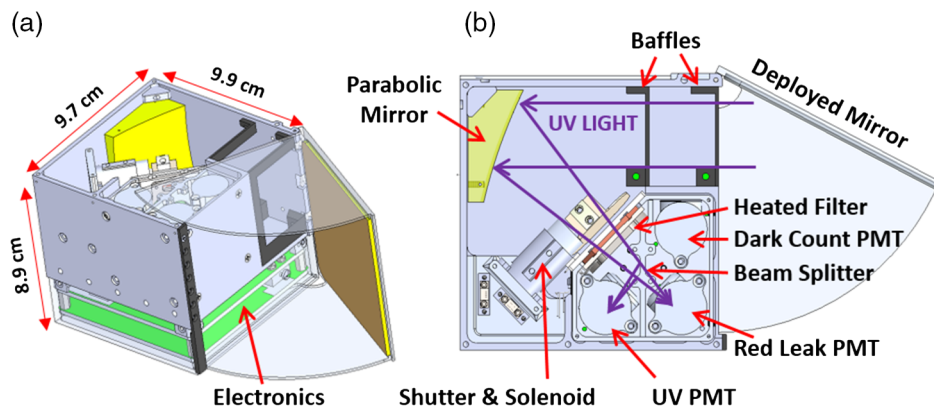


Fig. 1 Internal components of a Tri-TIP instrument (from Ref. 12): (a) isometric view of the instrument to indicate overall dimensions and the location of the sensor electronics and (b) top view illustrating the optical path and general internal layout. Incoming UV light passes through two simple baffles and onto an OAP mirror. Light is focused through the heated filter and divided at the beam splitter between two PMTs at the prime focus, a red leak PMT and a UV PMT. The dark count PMT is totally enclosed to seal out all light but measures dark counts due to high energy particles on-orbit. The deployable mirror is on the inside face of the hinged dust cover door and is used to select the instrument's viewing direction. The shutter and solenoid assembly blocks incoming light to protect the instrument should it inadvertently view the Sun as detected by a Sun sensor embedded in the electronics (not shown).

SrF₂ filter above 90°C shifts the shortwave cutoff wavelength to a point between 130.4 and 135.6 nm, eliminating unwanted bright nightglow signatures from atomic hydrogen (H α 121.6 nm) and atomic oxygen (O α 130.4 nm).^{6,17} The remaining light is then divided at the beam splitter, with half of the beam directed to the UV PMT and the other half directed toward the red leak PMT.

The Tri-TIP detectors are commercial Hamamatsu R13194 PMTs with a peak response at 130 nm.¹⁸ Each PMT within the Tri-TIP has a separate function, and all three constitute a matched set to ensure the highest accuracy measurement of the 135.6-nm emission.¹⁴ The dark count PMT is sealed from all light to measure background noise in the system. In a nominal Tri-TIP configuration, the UV PMT measures the desired signal (O α 135.6 nm) along with any parasitic longer wavelength radiation present in the signal. The red leak PMT sits behind a Hemlux, VUV grade sapphire (Al₂O₃) substrate beam splitter with a sharp cutoff at 140 nm to measure the long-wavelength background signal for later subtraction from the UV PMT signal.¹³

The second Tri-TIP configuration uses a VUV-grade MgF₂ substrate beam splitter that divides the incoming signal more evenly and effectively turns the red leak PMT into a second UV PMT.¹⁵ PMT covers at the focus of the OAP are positioned to select different field points and define the spatial resolution (0.2 deg vertical \times 7.25 deg across track) within the field of regard. When pointed above the limb of the Earth, the PMTs with slits will measure two narrowly separated altitudes simultaneously within the same instrumental field-of-view (3 deg \times 7.25 deg across track). This will be referred to as the limb configuration of Tri-TIP because the approach is only feasible when the instrument is pointed at tangent heights above the cloud layer of the Earth, where red leak correction is not needed.

Figure 2 shows examples of two Tri-TIP beam splitters in the bottom left corner. A reflective Acton #1300 AlMgF₂ coating is deposited on the surface in a polka-dot pattern to minimize geometric effects of the reflective pattern in any preferential direction. Dots with a 1.197-mm diameter were applied separated by a center-to-center distance of 1.5 mm to provide 50% surface area coverage. Both the nominal and the limb configuration beam splitters use the same AlMgF₂ reflective coating as the OAP, which is 75% reflective at a 45 deg angle of incidence at 135.6 nm (see Fig. 3).¹⁶ The reflectivity of the AlMgF₂ coating has shown measurable angular dependence, although the effects are small for angles of incidence near 45 deg from surface normal as used for Tri-TIP.¹⁹ The coating was deposited on the substrates by vacuum evaporation using a laser cut mask to generate the reflective pattern.

Figure 2 also shows the laboratory sample holder in the top left corner, which was used to test multiple beam splitters for the Tri-TIP instrument. The test bracket was mounted on a vacuum-compatible linear translation stage at 45 deg relative to the incoming UV beam. Figure 2

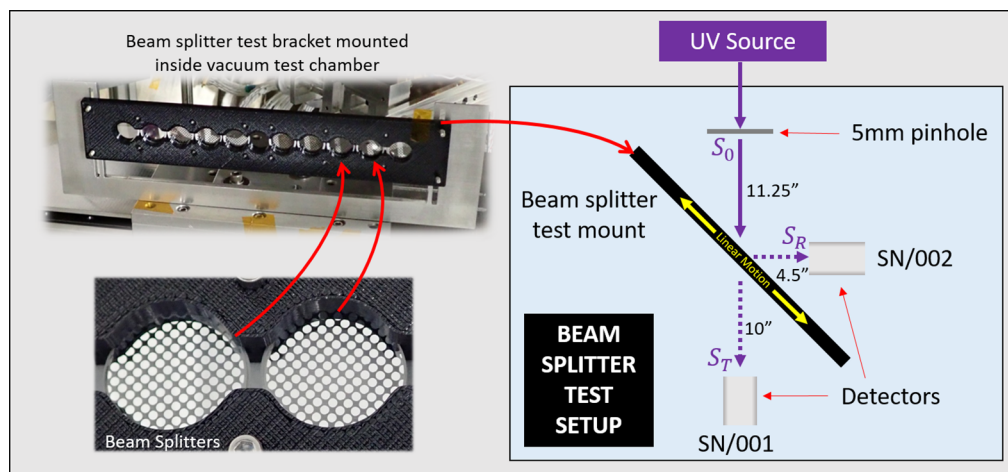


Fig. 2 Two Tri-TIP beam splitters are shown (bottom left) as they appear in the test sample holder. Beam splitters are 2-mm thick and 20 mm in diameter. The reflective coating provides 50% coverage of the substrate with a reflective coating.¹⁶ The test bracket (top left) is mounted on an adjustable stand and translation stage inside the vacuum test chamber. A schematic diagram of the test setup (right) illustrates the position of the test bracket relative to the reference detectors.

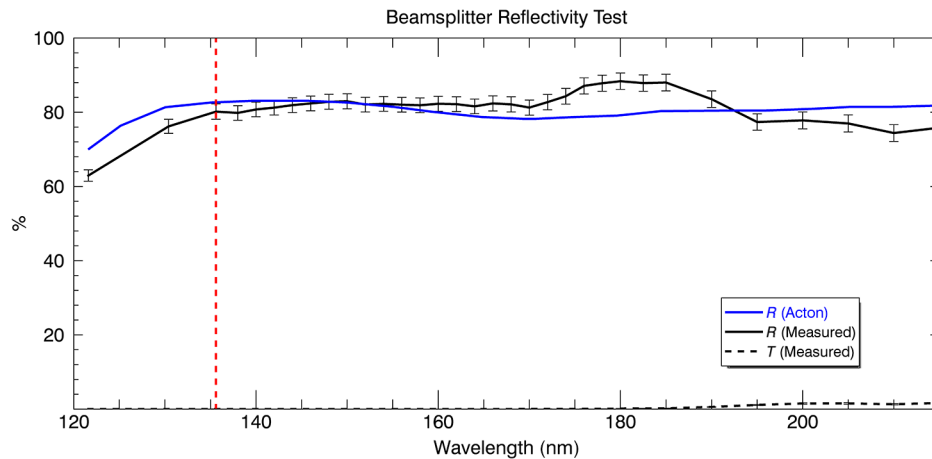


Fig. 3 Comparison of reflectivity (R) and transmissivity (T) for the AlMgF₂ coating witness sample (black) with the reflectance data values provided by the manufacturer (blue).¹⁶ 135.6 nm is indicated by the red-dashed line.

additionally shows a figure illustrating the test configuration within the vacuum chamber. The transmissivity and reflectivity of the beam splitters were measured using a pair of cross-calibrated, CsI PMTs. The tests were conducted using the Ultraviolet Calibration and Testing Facility maintained within the NRL Space Science Division. The UV light was produced using a hollow-cathode gas discharge source feeding a 1-m McPherson grazing-incidence monochromator and then sent through an exit slit into the test chamber.²⁰ Light was collimated inside the chamber by two plates with 5-mm diameter apertures and separated by 50 cm. The 5-mm diameter was chosen to deliberately underfill both the beam splitter surface and the active area of the calibrated laboratory PMTs.

3 Methodology

The bracket shown in Fig. 2 held 10 samples for test. One position was left open in the center of the bracket for baseline measurements of the light source, S_0 . The collimated 5-mm beam was incident on the beam splitter at 45 deg, and the resultant two beams were centered on the two-measurement PMTs. Measurements were made by alternating between each beam splitter and the open aperture in the test fixture to determine S_T and S_0 , both obtained by PMT SN/001 shown in Fig. 2. The transmissivity, T , was calculated simply as follows:

$$T = \frac{S_T}{S_0}, \quad (1)$$

where S_T is the number of counts measured as transmitted through the sample and S_0 is the average number of counts measured directly in the open sample position by the transmissivity detector (PMT SN/001 in Fig. 2) both before and after measuring S_T . Similarly, the reflectivity, R , was calculated as follows:

$$R = \frac{S_R}{S_0 G(\lambda)}, \quad (2)$$

where S_R is the number of counts measured by the detector positioned to measure the reflected part of the beam (PMT SN/002 in Fig. 2). Differences in detector responsivity as a function of wavelength are accounted for in $G(\lambda)$, the detector cross-calibration determined in a separate test prior to evaluation of the beam splitters. The transmissivity and reflectivity were both measured for each sample across a range of wavelengths, from 121.6 to 215 nm, at varying intervals.

The test integration time was selected at each wavelength to ensure that sufficient counts were acquired such that error from counting statistics were <1%. Systematic uncertainty due

to cross-calibration in the laboratory detectors is the dominant error in the following results, but the total is still $<3\%$. Error bars in all of the following plots reflect Poisson (counting) statistics in the experimental measurement (δS_T , δS_R , and δS_0) as well as systematic uncertainty due to the cross-calibration of reference detectors. A system-level test of Tri-TIP will be conducted in preparation for flight to determine the overall sensitivity and signal-to-noise ratio of the instrument.

Substrates for each material (VUV-grade Al_2O_3 or MgF_2) were all cut from the same respective boule, with each sample being 2-mm thick and 20 mm in diameter. The surface coating pattern was applied to each sample using a set of identical, laser-cut masks. The variability in measured signals between samples due to the polka-dot pattern was expected to be minimal for a 5-mm diameter beam. The small uncertainty introduced by the positional uncertainty of the beam on the polka-dot pattern was determined by ray trace calculations and verified by spatial scans across the surface of each sample, as presented in Sec. 4. A coated but unpatterned witness sample was also produced by the coating laboratory during each coating run and the vendor provided reflectance data for these.¹⁶ Witness substrates were drawn from the same lots as the beam splitters, so their reflectivity provides a basis for comparison to the patterned samples which, along with prior tests of uncoated filter substrates, allows for verification of the fractional coverage by the polka-dot pattern.^{6,12}

4 Results

The reflectivity of the fully coated MgF_2 witness substrate was measured as a function of wavelength to first verify the reflectivity of the coating. Figure 3 compares the results of the laboratory tested reflectivity (black line with error bars) to the manufacturer data sheet for the coated samples (blue line).¹⁶ A red dashed line is included at 135.6 nm to locate the wavelength of primary interest in the Tri-TIP.

The manufacturer reflectance curve shows a fairly flat response through the region of interest longward of 140 nm, and the reflectance decreases at wavelengths shorter than 130 nm. The test results agree with the manufacturer data, particularly close to 135.6 nm. At wavelengths greater than 180 nm, a small signal was measured by the transmissivity detector (PMT SN/001) due to low-level scattered light within the vacuum chamber (black dashed line), though the effects are less than the 3% system uncertainty in the measurement.

A Zemax Monte Carlo calculation was made to simulate the effect of the reflective mask geometric pattern on the measured signal. The simulation was initiated by passing 500,000 randomly located rays from a 5-mm diameter source through the beam splitter reflective pattern. A grid of reflective circles (diameter = 1.197 mm) was arranged in a layout identical to the Tri-TIP beam splitter polka-dot mask (center spacing 1.50 mm) oriented at 45 deg. The simulated rays were sent toward the surface at 45 deg to the surface normal to simulate the orientation of the beam splitter within the test (and Tri-TIP) configuration. The Monte Carlo calculation was repeated at a grid of positions to cover the full period of the polka-dot pattern in both X and Y directions in stepwise increments of 0.1 mm. Figure 4 shows the results of one simulated linear scan of a beam across the beam splitter (blue line), represented as the ratio of rays reflected off the mask to the number of rays that passed through the mask (R/T). A periodic modulation of the signal is shown in Fig. 4 as the 5-mm circular beam passes over the 1.5-mm periodic polka-dot pattern.

The geometric effect of the polka-dot reflective coating was tested on one sapphire beam splitter sample, as shown in Fig. 2. Figure 4 shows the ratio between the measured reflectivity and transmissivity as a function of position (black diamonds). Since the sample beam of 5-mm diameter does not span an exact multiple of the 1.5-mm dot pattern, a small modulation of the reflected signal is expected as the beam splitter is moved with respect to the 5-mm sample. To measure this experimentally, the beam splitter was moved through the fixed UV source beam in increments of 0.2 mm until the signal fell off at the edge of the sample in either direction. Several measured periods were averaged together to smooth out small variations due to minute imperfections in the reflective coating, and the result was centered on the peak ratio.

The test results agree well with the prediction of the Monte Carlo simulation. The variability in R/T over one period of the polka-dot pattern is ± 0.05 for a 5-mm diameter incident beam. The

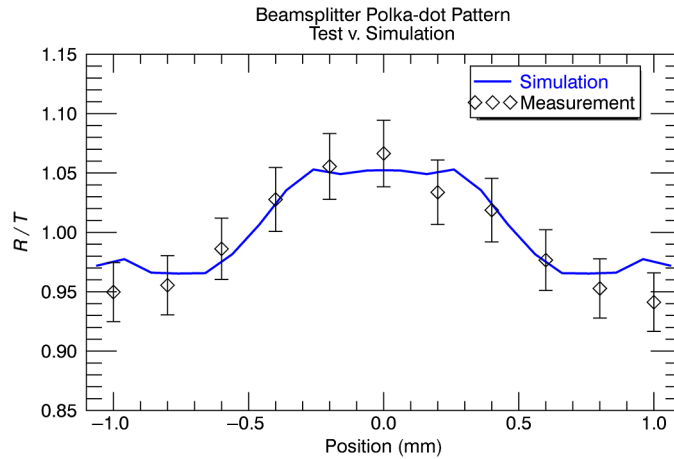


Fig. 4 The blue line shows the simulation of scanning the polka-dot mask in 0.1 mm increments for variability due to geometric effects. Black diamonds show the average of four test results scanning across a polka-dot mask for signal variability. Both values represent the ratio of reflectivity to transmissivity (R/T) seen as a 5-mm diameter source moves relative to the polka-dot beam splitter pattern, which has a periodicity of 1.5 mm. The travel required to span one period of the pattern at 45 deg is 2.12 mm.

periodic modulation will be further reduced with the larger operational Tri-TIP illumination footprint that covers more periods of the reflective pattern in both directions. The parabolic mirror generates a trapezoidal illumination pattern in the focal plane, and that pattern is larger at the beam splitter location because the light is unfocused prior to reaching the PMT at the focal plane. At the beam splitter, the total illumination covers an area roughly 15 mm × 10 mm, more than seven times the area of the laboratory test beam.

4.1 Sapphire Beam Splitter

Test results for three sapphire substrate beam splitters are shown in Fig. 5. The plot shows both reflectivity (R) and transmissivity (T) for all three samples (S1, S2, and S3). Colors are used to match results for each sample (black, blue, and green). Solid lines represent reflectivity and dashed lines represent transmissivity.

The reflectivity of all three samples is similar throughout the FUV region, particularly at 135.6 nm, and remains roughly constant longward of 140 nm. The wavelength dependence

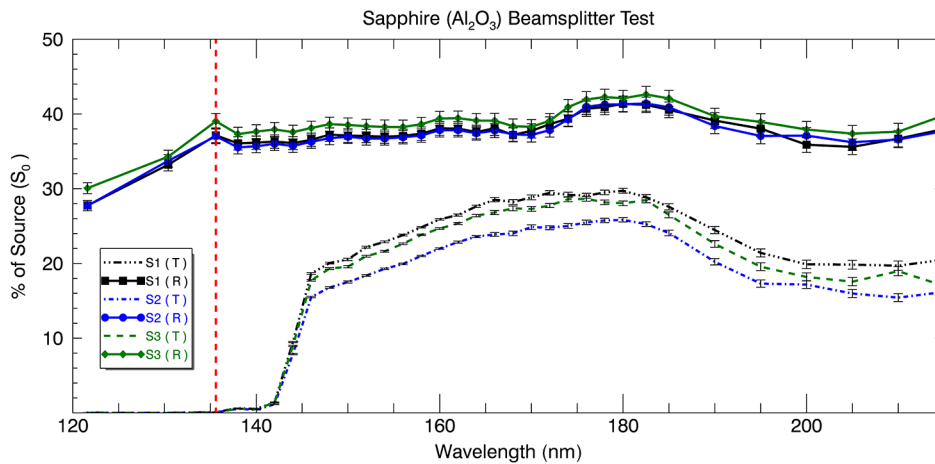


Fig. 5 Reflectivity (R) and transmissivity (T) of three sapphire substrate (Al_2O_3) polka-dot beam splitter samples (S1, S2, and S3) for use in the nominal Tri-TIP configuration. Solid lines represent reflectivity, and dashed lines represent transmissivity. The dashed red line is located at 135.6 nm.

Table 1 Summary of performance for beam splitters used in Tri-TIP.

Material wavelength	Al ₂ O ₃ 135.6 nm	Al ₂ O ₃ 200 nm	MgF ₂ 135.6 nm	MgF ₂ 200 nm
Index of refraction (<i>n</i>)	>2.0 ²¹	1.91 ²¹	1.57 ²²	1.42 ²²
Polka-dot mask (μ_{mask})	0.5	0.5	0.5	0.5
Substrate attenuation (μ_{atten})	1.0	0.5 ⁶	0.35 ²³	0.08 ²³
Surface reflection (μ_{Fresnel})	0.27	0.16	0.06	0.08
<i>T</i> (calculated)	0.0 <i>S</i> ₀	0.21 <i>S</i> ₀	0.31 <i>S</i> ₀	0.42 <i>S</i> ₀
<i>T</i> (experimental)	0.0 <i>S</i> ₀	0.20 <i>S</i> ₀	0.25 <i>S</i> ₀	0.35 <i>S</i> ₀
<i>R</i> (experimental)	0.38 <i>S</i> ₀	0.38 <i>S</i> ₀	0.34 <i>S</i> ₀	0.35 <i>S</i> ₀

of the reflectivity matches well that of the fully coated test sample, as shown in Fig. 3. The nominal reflectance level of the beam splitter samples agrees with the fully coated sample as well, which showed $\approx 80\%$ reflectivity at 135.6 nm. The polka-dot pattern results in half of the total signal being reflected or $\approx 40\%$ of the overall total beam.

The transmissivity of the sapphire substrate is zero below 135.6 nm, as desired. At longer wavelengths, the transmissivity varies more between samples than does the reflectivity, but the samples still show a high degree of similarity. At 200 nm and 45 deg to the surface normal, the sapphire substrate will reflect $\approx 11\%$ of light at each surface, as determined by the Fresnel equations for reflectivity. Half of the total signal (*S*₀) is blocked by the polka-dot pattern ($\mu_{\text{mask}} = 0.5$) and is then further attenuated by $\approx 50\%$ due to absorption ($\mu_{\text{atten}} = 0.5$) in the sapphire substrate.⁶ Finally, $\approx 16\%$ of unpolarized light is lost due to all combined surface reflections within the substrate. The expected transmission with all expected losses accounted for is $0.21S_0$. The test shows that $\approx 20\%$ of the total signal passes through the beam splitter at 200 nm, which matches the expected transmission. Table 1 summarizes the data used in the calculations, with values listed for both 135.6 and 200 nm for comparison.

4.2 Limb Beam Splitter

Figure 6 shows the test results for two limb (MgF₂ substrate) beam splitter samples (S1 and S2) with colors again used to pair results for the same sample (black, blue). The reflectivity is shown with the solid lines and the transmissivity by the dashed lines, with a red dashed line to locate 135.6 nm.

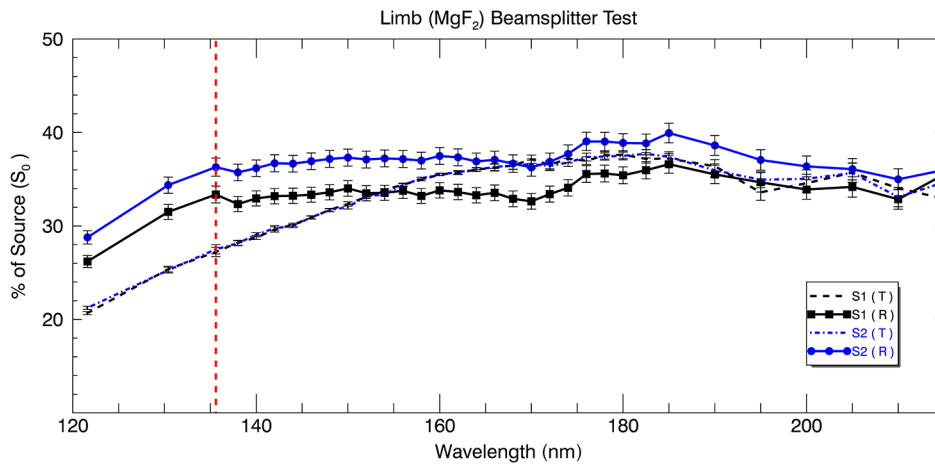


Fig. 6 Reflectivity (*R*) and transmissivity (*T*) of two MgF₂-substrate polka-dot beam splitter samples (S1 and S2) for use in the limb Tri-TIP configuration. Solid lines represent reflectivity, and dashed lines represent transmissivity. The dashed red line represents 135.6 nm for reference.

The reflectivity curves for each sample show an agreement in their wavelength dependence, with slightly more variation in total reflectivity between samples than was seen for the sapphire beam splitters. The transmissivity, on the other hand, is nearly identical for both S1 and S2. At 135.6 nm, the transmissivity is $\approx 25\%$, as expected based on prior tests.⁶ The signal (S_0) will be attenuated due to absorption in the MgF_2 substrate (μ_{atten}) and due to internal surface reflections within the substrate (μ_{Fresnel}) using an index of refraction, $n_M = 1.56568$, for MgF_2 at 135.6 nm.²² With the expected values for attenuation, the expected transmitted signal is $0.31S_0$, which is slightly higher than the measured transmissivity but still within acceptable agreement.

The optical test results described in both prior and present tests can be used to illustrate the expected effects of the FUV optical path through Tri-TIP.⁶ Figure 7 shows data from the Ultraviolet Limb Imaging experiment in panel 1, which included a FUV (108 – 180 nm) spectrometer with 0.6-nm resolution.²⁴ The dayglow spectrum was measured on May 5, 1991, at 23:29:11 UT and the nightglow spectrum was measured on May 4, 1991, at 7:33:05 UT. These data represent typical dayglow and nightglow spectra and are presented as a means to illustrate the data analysis methodology of Tri-TIP and highlight the role the beam splitter plays. The Tri-TIP is designed with only the nightglow (purple trace) in mind, though the dayglow spectrum (black dashed line) is included to help illustrate structure in the Earth's airglow FUV spectrum.

Panel 2 in Fig. 7 shows the fractional emission that would be measured by the Tri-TIP PMT after only a single reflection from the OAP. This fractional spectrum and all that follow have been normalized to the peak at 135.6 nm for comparison. Panel 3 shows the effect of the SrF_2 filter on the spectra, which is effectively what the UV PMT will measure spectrally. Panel 4 shows the signal that will be measured by the red leak PMT for later subtraction from the UV PMT measurement (i.e., panel 3). Finally, panel 5 shows the expected final output after the red leak correction has been taken into account. The dayglow spectrum still contains residual emission from other atmospheric species (e.g., N_2 LBH band emission), but the nightglow spectrum is left with only the desired OI 135.6-nm emission line.

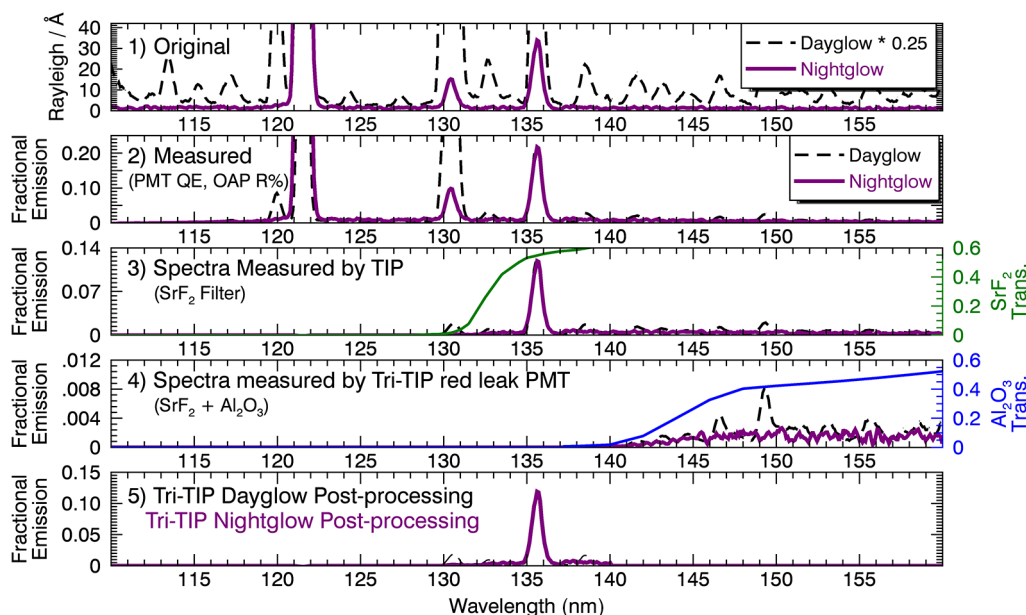


Fig. 7 Optical effects of the Tri-TIP instrument are illustrated using both dayglow and nightglow spectra. Panel 1 shows sample airglow data provided by the Ultraviolet Limb Imaging experiment (see text for further details).²⁴ Panel 2 shows the spectra that would be measured by the PMT without any filters in place, with both spectra normalized to the peak at 135.6 nm for structural comparison. Panel 3 shows the effect of adding the heated SrF_2 filter to the optical path, as was done for TIP. Panel 4 shows what the red leak PMT in Tri-TIP will measure after passing through the Al_2O_3 beam splitter. Panel 5 shows the final output of the Tri-TIP instrument after the final postprocessing of the data.

5 Summary

Mechanically simple, passive optical systems capable of isolating signals may be useful for future CubeSat missions that wish to use photometric UV observations. Photometry is a remote sensing approach that achieves high sensitivity measurements of UV signals from small optical packages, which is enabled by shorter path lengths due to a lack of dispersive gratings. The TIP instrument has demonstrated the ability to meet required 99% rejection levels at 130.4 nm (and any other emissions at shorter wavelengths) with a preflight sensitivity well above the mission requirement.^{6,9} Tri-TIP fits a multiphotometer spaceflight system based on TIP for ionospheric remote sensing into a 1U CubeSat instrument (10 cm × 10 cm × 10 cm) capable of achieving a required sensitivity of 150 cts/s/R while improving measurement cadence over the legacy TIP instruments.⁷ The key enabling technology in the Tri-TIP is the VUV polka-dot beam splitter that has been tested to demonstrate the functionality necessary to meet the Tri-TIP mission requirements.

The Tri-TIP beam splitter has been successfully applied to two separate configurations of CubeSat instruments, and both configurations of the Tri-TIP instrument will be used as part of the CIRCE mission.⁴ The beam splitter in the nominal Tri-TIP configuration will enable the accurate determination of OI 135.6-nm emissions in the nighttime ionosphere along the nadir-viewing ground track of the spacecraft by simultaneously measuring long wavelength contamination to be later removed from the signal. The limb Tri-TIP configuration will enable the simultaneous measurement of OI 135.6 nm at two adjacent tangent heights above the limb of the Earth within a single optical system. The CIRCE mission objective is to use the two-dimensional reconstructions of the ionosphere to characterize distributions of electrons in the orbital plane of the spacecraft, particularly in the equatorial region. The data collected by the Tri-TIP instruments will enable tomographic reconstruction of nightglow in the nightside ionosphere using optically thin OI 135.6-nm emissions, which will be used to determine electron distributions in the ionosphere.

Acknowledgments

B.A.F. is an NRC postdoctoral research associate at the US Naval Research Laboratory (NRL). Work at NRL for all authors is supported by the chief of Naval Research. B.A.F. would like to thank Dr. R. R. Meier for his helpful suggestions in the preparation of the analysis in this manuscript.

References

1. M. Zukic and D. G. Torr, "Multiple reflectors as narrow-band and broadband vacuum ultraviolet filters," *Appl. Opt.* **31**, 1588–1596 (1992).
2. L. R. de Marcos et al., "Narrowband filters for the FUV range," *Proc. SPIE* **9510**, 95100J (2015).
3. R. R. Meier, "Ultraviolet spectroscopy and remote sensing of the upper atmosphere," *Space Sci. Rev.* **58**, 1–185 (1991).
4. K. F. Dymond et al., "The Tiny Ionospheric Photometer (TIP) on the constellation observing system for meteorology, ionosphere, and climate (COSMIC/FORMOSAT-3)," *J. Geophys. Res. A Space Phys.* **121**, 10,614–10,622 (2016).
5. S. A. Budzien et al., "Tiny Ionospheric Photometers on FORMOSAT-3/COSMIC: on-orbit performance," *Proc. SPIE* **7438**, 743813 (2009).
6. A. W. Stephan et al., "Evaluation of UV optics for Triple Tiny Ionospheric Photometers on CubeSat missions," *Proc. SPIE* **10769**, 107690W (2018).
7. P. C. Kalmanson et al., "The Tiny Ionospheric Photometer instrument design and operation," *Proc. SPIE* **5660**, 259 (2004).
8. G. R. Carruthers, "Mesh-based semitransparent photocathodes," *Appl. Opt.* **14**, 1667–1672 (1975).
9. K. F. Dymond et al., "On-orbit calibration of the Tiny Ionospheric Photometer on the COSMIC/FORMOSAT-3 satellites," *Proc. SPIE* **7438**, 743814 (2009).

10. A. S. Tremsin and O. H. W. Siegmund, "UV radiation resistance and solar blindness of CsI and KBr photocathodes," *IEEE Trans. Nucl. Sci.* **48**, 421–425 (2001).
11. A. W. Stephan et al., "LITES and GROUP-C: multi-sensor ionospheric imaging from the ISS," *Proc. SPIE* **9222**, 92220M (2014).
12. K. F. Dymond et al., "Low-latitude ionospheric research using the CIRCE Mission: instrumentation overview," *Proc. SPIE* **10397**, 1039719 (2017).
13. GT Crystal Systems, *Hemlux LAOS 193 VUV Grade Sapphire*, Salem, Massachusetts (2018).
14. S. A. Budzien et al., "Three-channel airglow photometer data analysis methodology," Technical Report, US Naval Research Laboratory, Washington, DC (2018).
15. Crystran Ltd., *VUV Grade MgF₂*, Poole, England (2018).
16. Acton Research Corporation, "CAMS—deep UV," PN#1300-FR30-FoldAllow (2018).
17. T. Tomiki and T. Miyata, "Optical studies of alkali fluorides and alkaline earth fluorides in VUV region," *J. Phys. Soc. Jpn.* **27**(3), 658–678 (1969).
18. Hamamatsu Corporation, "R13194 photomultiplier tube," USA Headquarters, Bridgewater, New Jersey (2015).
19. W. R. Hunter, J. F. Osantowski, and G. Hass, "Reflectance of aluminum overcoated with MgF₂ and LiF in the wavelength region from 1600 Å to 300 Å at various angles of incidence," *Appl. Opt.* **10**, 540–544 (1971).
20. F. Paresce, S. Kumar, and C. S. Bowyer, "Continuous discharge line source for the extreme ultraviolet," *Appl. Opt.* **10**, 1904–1908 (1971).
21. F. Gervais, "Aluminum oxide (Al₂O₃)," in *Handbook of Optical Constants of Solids*, E. D. Palik, Ed., pp. 761–775, Academic Press, Burlington (1997).
22. T. M. Cotter, M. E. Thomas, and W. J. Tropsf, "Magnesium fluoride (MgF₂)," in *Handbook of Optical Constants of Solids*, E. D. Palik, Ed., pp. 899–918, Academic Press, Burlington (1997).
23. M. A. Quijada, J. D. Hoyo, and S. Rice, "Enhanced far-ultraviolet reflectance of MgF₂ and LiF over-coated Al mirrors," *Proc. SPIE* **9144**, 91444G (2014).
24. S. A. Budzien, P. D. Feldman, and R. R. Conway, "Observations of the far ultraviolet airglow by the ultraviolet limb imaging experiment on STS-39," *J. Geophys. Res. A Space Phys.* **99**, 23275–23287 (1994).

Bruce A. Fritz is an NRC postdoctoral research associate in the Space Science Division at the U.S. Naval Research Laboratory, Washington, DC. His research interests include ultraviolet remote sensing of the high latitude ionosphere and thermosphere. His recent work includes investigation of neutral upwelling in the cusp region using photometer measurements from the Rocket Experiment for Neutral Upwelling 2 sounding rocket experiment and the Special Sensor Ultraviolet Limb Imager on the DMSP spacecraft.

Andrew W. Stephan is a research physicist at the U.S. Naval Research Laboratory. He received his BS degrees in physics and mathematics from the University of Wisconsin and his MA and PhD degrees in astronomy from Boston University. His primary research interest is in the remote sensing of Earth's upper atmosphere and space environment, with an emphasis on the ultraviolet airglow and aurora produced in the ionosphere and thermosphere.

Charles M. Brown received his PhD in chemical physics in 1971. Since then, he has been a physicist in the NRL Space Science Division. His specialty is spectroscopy and he has contributed to 15 space flight instruments including MAHRSI on the shuttle, BCS and EIS on Japanese satellites. He has studied laboratory spectra of atoms and plasmas and x-ray and EUV spectra from the Sun. He is working with SHS instruments REDDI and MIGHTI to measure upper atmospheric winds, and the CIRCE CubeSat for ionospheric studies. He is a fellow of the Optical Society of America.

Biographies of the other authors are not available.